

Scheduling Deep Learning Jobs in Multi-Tenant GPU Clusters via Wise Resource Sharing

Yizhou Luo*, Qiang Wang[†], Shaohuai Shi[†], Jiaxin Lai*, Shuhan Qi[†], Jiajia Zhang[†], Xuan Wang[†]
Harbin Institute of Technology (Shenzhen)

Guangdong Provincial Key Laboratory of Novel Security Intelligence Technologies

*{23S151149,200110515}@stu.hit.edu.cn, [†]{qiang.wang,shaohuais,shuhanqi,zhangjiajia,wangxuan}@hit.edu.cn

Abstract—Deep learning (DL) has demonstrated significant success across diverse fields, leading to the construction of dedicated GPU accelerators within GPU clusters for high-quality training services. Efficient scheduler designs for such clusters are vital to reduce operational costs and enhance resource utilization. While recent schedulers have shown impressive performance in optimizing DL job performance and cluster utilization through periodic reallocation or selection of GPU resources, they also encounter challenges such as preemption and migration overhead, along with potential DL accuracy degradation. Nonetheless, few explore the potential benefits of GPU sharing to improve resource utilization and reduce job queuing times.

Motivated by these insights, we present a job scheduling model allowing multiple jobs to share the same set of GPUs without altering job training settings. We introduce SJF-BSBF (shortest job first with best sharing benefit first), a straightforward yet effective heuristic scheduling algorithm. SJF-BSBF intelligently selects job pairs for GPU resource sharing and runtime settings (sub-batch size and scheduling time point) to optimize overall performance while ensuring DL convergence accuracy through gradient accumulation. In experiments with both physical DL workloads and trace-driven simulations, even as a preemption-free policy, SJF-BSBF reduces the average job completion time by 27-33% relative to the state-of-the-art preemptive DL schedulers. Moreover, SJF-BSBF can wisely determine the optimal resource sharing settings, such as the sharing time point and sub-batch size for gradient accumulation, outperforming the aggressive GPU sharing approach (baseline SJF-FFS policy) by up to 17% in large-scale traces.

Index Terms—Distributed Deep Learning, Job Scheduling, Communication Contention

I. INTRODUCTION

The popularity of Deep Neural Network (DNN) [1] grows rapidly in both industry and academia with its significant role in various applications, such as computer vision and natural language processing. With more and more training data and larger model size, training deep models becomes very time-consuming. Distributed Deep Learning (DDL) [2] is widely adopted to speed up the training procedure, which distributes the training workload to a cluster of workers and exploit the parallel computing power to accelerate the training process.

In the data center scenario where the hardware resources are shared by multiple users, multiple online DDL training jobs are running simultaneously, and the resource contention could lead to severe performance degradation if the training

jobs are not scheduled properly [3]. For such an online scheduling system that concurrently handles a rising number of jobs, flexible resource allocation and efficient job scheduling are indispensable to maximize the resource utilization. There exist some traditional schedulers [4]–[8] to schedule different computing tasks, but they are not specifically designed for DDL training jobs and cannot leverage the characteristics of DDL (such as iterativeness and convergence properties) for maximal training efficiency.

Existing DL job management and scheduling systems [9]–[14] commonly employ preemptive and exclusive strategies to enhance system utilization and minimize job completion time. The advanced heuristic scheduler Tiresias [13] demonstrated that the shortest-remaining-service-first (SRSF) algorithm generally yields optimal results when job durations are known. However, small jobs still experience delays waiting for GPU resource release when the cluster is predominantly occupied by large jobs. The state-of-the-art representative is Pollux [15], which dynamically (re-)assigns resources to improve cluster-wide goodput, while respecting fairness and continually optimizing each DL job to better utilize those resources. However, Pollux helps users choose the GPU resources as well as tune the training hyper-parameters, which may result in model accuracy degradation [16]. Overall speaking, in preemptive and exclusive policies, long-term job packing can exacerbate HOL (Head-of-line) blocking issues and prolong JCT (Job Completion Time). Consequently, jobs with small training iterations and low GPU demand may face severe queuing and starvation issues, while those large ones can suffer from high migration overhead.

In several recent schedulers, including Gandiva [17], Zico [18], Salus [19] and Lucid [20], there has been a notable shift towards emphasizing resource sharing, particularly regarding GPU and network resources. This shift aims to enhance overall resource utilization while addressing queuing and starvation issues effectively. Gandiva [17] introduced GPU time-slicing and job scheduling based on predicted DDL training job characteristics, albeit with a conservative approach limiting GPU sharing to single-GPU jobs. Yu et al. [21], [22] tackled network resource sharing in multiple all-reduce based DDL job training, reducing communication contention overhead. Lucid [20] utilized an indolent packing strategy to mitigate interference effectively. However, their search was confined to

a limited solution space due to the inability to alter the training batch size.

On the contrary, gradient accumulation has become standard feature in many deep learning training frameworks [23]. The basic idea of gradient accumulation is to accumulate gradients from multiple micro-batches and only then update the model parameters. This is particularly helpful in training very large neural networks [24], where workers can only fit one small micro-batch at a given time, saving GPU memory footprint requirement. From an optimization perspective, gradient accumulation is completely equivalent to training with a larger mini-batch size, since in both cases the gradient is averaged with respect to all computed examples.

Motivated by the observations outlined above, we introduce a job scheduling model that enables multiple jobs to run concurrently on one or more GPUs. In contrast to the approach of scaling the training batch size and tuning training hyper-parameters as in [15], we investigate the potential of GPU sharing to improve the overall performance. This model is coupled with gradient accumulation to address GPU memory limitations and ensure model convergence. The contributions of this paper can be summarized as follows:

- We introduce a novel DDL job scheduling model enabling multiple jobs to fully or partially share the same set of GPUs while ensuring model convergence through gradient accumulation. Unlike existing methods that increase batch size and GPU numbers to enhance performance, risking accuracy degradation, our model focuses on GPU resource sharing across jobs and mitigates GPU memory constraints through gradient accumulation, thereby potentially reducing queuing time for waiting DDL jobs.
- We propose SJF-BSBF (shortest job first with best sharing benefit first), a straightforward yet effective scheduling algorithm for the aforementioned problem. Initially, we derive the optimal solution for scheduling a job pair (one ongoing job and one new arrival) to decide GPU sharing feasibility and launch timing. Subsequently, we employ a greedy strategy to determine batch size and GPU allocation, minimizing interference with existing jobs and reducing queuing time.
- Through both physical and simulated experiments, we evaluate SJF-BSBF on different scales of job traces. Compared to recent DL schedulers such as Tirasias [13] and Pollux [15], SJF-BSBF reduces average job completion time by 27-33%. Additionally, compared to the first-fit GPU sharing approach for new arrival jobs, SJF-BSBF avoids those sharing decisions that may degrade the overall performance, surpassing it by up to 17%.

II. RELATED WORK

Scheduling DL training jobs has garnered significant interest recently. Research in this field primarily focuses on fully utilizing computing resources and allocating them effectively to achieve optimal efficiency in multi-tenant GPU computing environments. Here we discuss two categories: preemptive and exclusive schedulers, as well as non-preemptive schedulers.

Preemptive and Exclusive Schedulers. These schedulers possess the capability to interrupt or preempt a running job in order to allocate exclusive resources to another job with higher priority. This mechanism ensures that allocated resources remain inaccessible to other jobs while the current job is utilizing them, thereby fostering predictable resource usage patterns and mitigating interference between jobs. Early works such as Optimus [12] and Cynthia [25] relied on job time prediction, making simplistic assumptions about training convergence curves. Tirasias [13] addressed the severe resource starvation issue by proposing adaptive scheduling algorithms with effective job migration strategies. Other studies, such as Harmony [26] and Spear [27], leveraged deep reinforcement learning to provide efficient solutions aimed at minimizing average job completion time or makespans. Another line of research in DDL job scheduling algorithms relies on theoretical formulation and optimization, treating DDL job scheduling as constrained optimization problems. The recent state-of-the-art Pollux [15] dynamically reallocates resources to enhance cluster-wide throughput while ensuring fairness and continually optimizing each DL job to maximize resource utilization. However, these methods cannot guarantee no accuracy degradation for all models. Moreover, they may encounter performance degradation due to migration [13] and GPU under-utilization [28].

Non-preemptive Schedulers. Early non-preemptive schedulers predominantly relied on heuristic algorithms based on job characterization and hardware performance modeling. In recent studies, attention has shifted towards resource sharing, encompassing GPU and network resources, which holds significant potential for improving computing resource utilization and alleviating starvation. Gandiva [17] introduced GPU time-slicing and job scheduling by predicting DDL training job characteristics. However, it adopted a conservative approach, limiting GPU sharing to single-GPU jobs. Zico [18] focused on system-wide memory consumption for concurrent training and devised a feasible memory management solution to ensure that concurrent jobs do not exceed the allocated memory budget. Wang et al. [29] and Yu et al. [21], [22] addressed network resource sharing in multiple ring-all-reduce based DDL job training, alleviating communication contention overhead. Lucid [20] employed an indolent packing strategy to mitigate interference. However, few of these approaches offer a general and flexible solution for sharing GPUs among DL jobs.

III. PRELIMINARIES

A. S-SGD Based Distributed Deep Learning

The DNN model is trained in an iterative manner with the target of minimizing a loss function $\mathcal{L}(W, D)$, where W and D are respectively the model weights and the input data. For large-scale DNNs, the data-parallel synchronized SGD (S-SGD) is widely applied to train models with multiple workers (say N workers, and indexed by g) because it has the same convergence performance as the sequential SGD. Generally the i^{th} iteration of the training contains four steps: a) Each worker g loads a mini-batch of local data D_i^g into the device

memory. b) Each worker g performs a feed forward on D_i^g through the neural network and computes the value of the loss function $\mathcal{L}(W_i, D_i^g)$. c) The first order gradients w.r.t. W_i are calculated by backpropagation. d) Gradients from all the workers $\nabla\mathcal{L}(W_i, D_i^g)$ are aggregated, averaged and then distributed, which is often tackled by the All-Reduce collective function. Then all the workers update the model as Eq. (1).

$$W_{i+1} = W_i - \xi \frac{1}{N} \sum_{g=1}^N \nabla\mathcal{L}(W_i, D_i^g). \quad (1)$$

B. All-Reduce Communication

The most common scenario of DDL training is using a large number of computing devices distributed among nodes in a cluster. As a result, the step d) involves extra communication overheads. In Eq. (1), we use $\Delta W_i = \frac{1}{N} \sum_{g=1}^N \nabla\mathcal{L}(W_i, D_i^g)$ to represent the aggregation of gradients from N workers, which can be done through an all-reduce operation or through a set of parameter servers. For brevity, we assume that the number of nodes is power-of-two. Given the number of nodes N and the message size M , the time cost of one All-Reduce operation without contention can be generalized as where a and b are two constant numbers that are not related to M [30]. The inter-node communication cost can be modelled as Eq. (2). The values of a and b depend on the algorithms for the All-Reduce operation with different number of processes and message sizes [30]. Without loss of generality, we do not limit the communication model to one specific algorithm.

$$T_{allreduce} = a + bM. \quad (2)$$

IV. SYSTEM MODELING AND PROBLEM FORMULATION

For ease of reference, we summarize some frequently used notations throughout this paper in Table I.

Table I
FREQUENTLY USED NOTATIONS

Name	Descriptions
\mathcal{S}/\mathcal{N}	Set of servers/GPUs in the cluster
S_i	the i -th server of the cluster
$g_{i,j}$	the j -th GPU on the i -th server
\mathcal{J}	The job set
G_j	# of GPUs requested by job j
J_k	the k -th job
$\mathcal{G}(J_k)$	the set of GPUs used by J_k
$\mathcal{S}(J_k)$	the set of servers used by J_k
a_k	the arrival time of J_k
B_k	the mini-batch size per-GPU used by J_k
I_k	# of iterations that J_k needs to run
t_k	The execution time of one iteration of J_k
L_k	The total execution time of J_k running solely
T_k	The completion time of job j
E_k	the timestamp when J_k is finished
\mathcal{F}	The set of feasible scheduling solution
f_j^k	The schedule of job j in the k -th solution

We consider a multi-tenant GPU cluster comprising $|\mathcal{S}|$ servers equipped with $|\mathcal{N}|$ GPUs evenly distributed. These servers are interconnected with a network switch possessing sufficient bandwidth. All GPUs within the cluster share the same specifications and theoretical peak performance. At the onset of a scheduling horizon $|\mathcal{T}|$ spanning time-slots, a set of

DDL jobs \mathcal{J} awaits scheduling for training over the duration of $|\mathcal{T}|$. Each job $J_k \in \mathcal{J}$ is characterized by the number of GPUs it requires, denoted as $\mathcal{G}(J_k)$, and the total number of training iterations I_k requested by its users.

A. DL Job Training Time Modeling

We first model the training time of one job, which includes the GPU computation time and network communication of the all-reduce operation.

1) *Modeling GPU Computation*: The DL model is trained using back-propagation. The computation time on GPU scales linearly with the per-GPU batch size B , which can be calculated as follows.

$$t_{comp}(B) = \alpha_{comp} + \beta_{comp} \times B. \quad (3)$$

2) *Modeling Network Communication*: The gradient aggregation overhead depends on the topology as well as the network communication algorithm. We simply define the communication part as follows.

$$t_{comm} = \alpha_{comm} + \beta_{comm} \times M, \quad (4)$$

where M is the message size, and $\alpha_{comm}, \beta_{comm}$ are the all-reduce time model parameters as described in Section III-B.

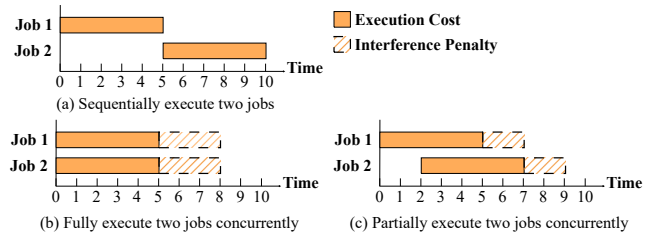


Figure 1. Three job schedules for two DL jobs.

3) *Sharing Performance Modeling*: Existing schedulers that facilitate GPU sharing, such as Gandiva [17], Gavel [14], and Lucid [20], often adopt conservative and limited approaches or require additional application information to generate schedules. In contrast, we apply a simple interference model to describe the overhead of GPU sharing. We illustrate three possible job schedules for two jobs sharing the same set of GPUs in Figure 1. Schedule (a) sequentially executes two DL jobs. Schedules (b) and (c) involve invoking two DL jobs simultaneously or with partial overlap, resulting in varying degrees of interference penalty. To optimize the average job completion time, one must balance the tradeoff between job queuing/waiting time (Job 2 waits for Job 1 to finish in (a)) and interference penalty (complete overlap of two jobs leads to severe penalty in (b)). In practice, the job iteration time under GPU sharing can be measured and modeled by equations (3) and (4), as they occupy partial GPU and network resources with similar trends. To simplify the model, if a new job shares

GPUs occupied by an existing job (Job A and Job B), we adjust their job iteration time as follows.

$$\hat{t}_A = t_A \xi_A, \quad (5)$$

$$\hat{t}_B = t_B \xi_B, \quad (6)$$

where ξ_A and ξ_B denote the interference ratios, reflecting the performance degradation resulting from GPU sharing. The solution to determining the optimal scheduling point under this scenario will be discussed in Section V-A.

4) *Modeling Gradient Accumulation*: Given that GPU memory constraints may limit the per-GPU batch size, some schedulers tackle this limitation through memory offloading [31] (which may introduce additional system overhead) or by adjusting batch sizes and other training hyper-parameters [15] (which may compromise model accuracy). As our model incorporates GPU sharing, the memory footprint frequently imposes constraints on feasibility. Thus, we focus on gradient accumulation, which can dynamically reduce the sub-batch size while preserving the original model accuracy as per the user’s requested batch size. It is also easily implemented using popular DL frameworks. It is important to note that one can utilize gradient accumulation algorithms to manage the computational aspect, thereby reducing batch size to mitigate memory consumption. We subsequently define the overall iteration time as follows.

$$t_{iter}^j = (s - 1) \times t_{comp}^j \left(\frac{B}{s}\right) + \left((t_{comp} \left(\frac{B}{s}\right))^\delta + t_{comm}^\delta \right)^{1/\delta}, \quad (7)$$

where s represents the accumulation step required to attain the original batch size, and δ denotes the degree of overlap between GPU computation and all-reduce communication, as initially proposed in [15]. It is important to acknowledge that δ may vary when different batch sizes are applied.

B. Scheduling Modeling

In this paper, we adopt the “gang-scheduling” discipline widely prevalent in practical large-scale GPU clusters [13], [22], [32]. Under gang scheduling, all workers (i.e., GPUs) of a DDL job must be allocated simultaneously. Furthermore, once a job commences its scheduled run, all allocated GPUs must remain dedicated to the job until its completion, with no allowances for preemption or migration. (It is worth noting that frequent job preemption and migration can significantly degrade performance [13]). Upon job completion, the occupied resources are simultaneously released. Differing from conventional GPU-exclusive scheduling policies, we permit GPUs to be occupied by multiple workers from various jobs concurrently. These workers can be allocated within a single server or across multiple servers, provided there exists a network path connecting them.

Assume $y_{jg}[\tau]$ denotes that the job j uses GPU g in the time slot t . Job j requires G_j number of GPUs.

$$\sum_{g \in \mathcal{G}} y_{jg}[\tau] = G_j. \quad (8)$$

To ensure that one GPU at most holds C jobs, we have

$$\sum_{j \in \mathcal{J}[\tau]} y_{jg}[\tau] \leq C, \forall j \in \mathcal{J}[\tau], \tau \in \mathcal{T}, g \in \mathcal{G}. \quad (9)$$

In practice, we observe that interference degradation can be severe, rarely improving performance when more than two jobs share the same set of GPUs. Therefore, we set $C = 2$ in our context.

Also, since we consider gang scheduling, we have

$$y_{jg}[\tau] = y_{gs}[\tau - 1], \forall s \in S, j \in \mathcal{J}[\tau], a_j < \tau \leq T_j, \quad (10)$$

$$y_{jg}[\tau] = 0, \forall g \in \mathcal{G}, j \notin \mathcal{J}[\tau], \tau \in \mathcal{T}, \quad (11)$$

$$y_{jg}[\tau] \in \mathbb{Z}^+, \forall g \in \mathcal{G}, j \in \mathcal{J}[\tau], \tau \in \mathcal{T}. \quad (12)$$

The completion time of job j can be calculated as

$$T_j = a_j + \arg \min_{\tau \in \mathcal{T}} \sum_{j \in \mathcal{J}[\tau]} \frac{1}{t_{iter}^j} \geq I_k, \forall j \in \mathcal{J}[\tau], \tau \geq a_j, \quad (13)$$

$$\phi_j[t] = \frac{B_k}{t_{iter}^j}, \quad (14)$$

where $\phi_j[\tau]$ denotes the system throughput of the job. In practice, it is more common to monitor and collect DL training throughput using popular DL frameworks. The throughput can be readily converted to iteration time given the training batch size. By measuring DL job throughput under both sole execution and concurrent execution with other jobs, we can fit the time model (Equation (7)) for both cases and naturally infer the interference ratio ξ . Figure 2 illustrates the throughputs of all DL models in our experiments across a range of resource allocations and batch sizes. Overall, our model closely represents the observed data. We also notice that different jobs exhibit varying sensitivities to network communication and GPU workloads. For instance, BERT shows a linear increase with batch size within the experimental range for all GPU configurations, indicating that the bottleneck lies in GPU computation and is constrained by GPU memory. Additionally, YoloV3 mostly achieves peak throughput with a batch size of 16 and encounters network bottlenecks when the GPU number exceeds 12. We also measure the system throughput of different job pairs and training configurations, as depicted in Figure 3. We find that throughput can be fitted by Equation (14), albeit with different parameters from the solely running mode. Moreover, the interference ratios of different cases exhibit a wide range of up to 6 in our experiments, emphasizing that avoiding unfavorable cases is crucial for improving overall performance.

C. Problem Formulation

In this paper, our goal is to determine the scheduling decisions $y_{jg}[t]$ to minimize the average JCT, which is commonly used to evaluate the efficiency of DL job schedulers [13], [15]. This optimization problem can be formulated as follows:

$$\min_{y_{jg}[t], \forall j, g, t} \sum_{j \in \mathcal{J}[t]} T_j. \quad (15)$$

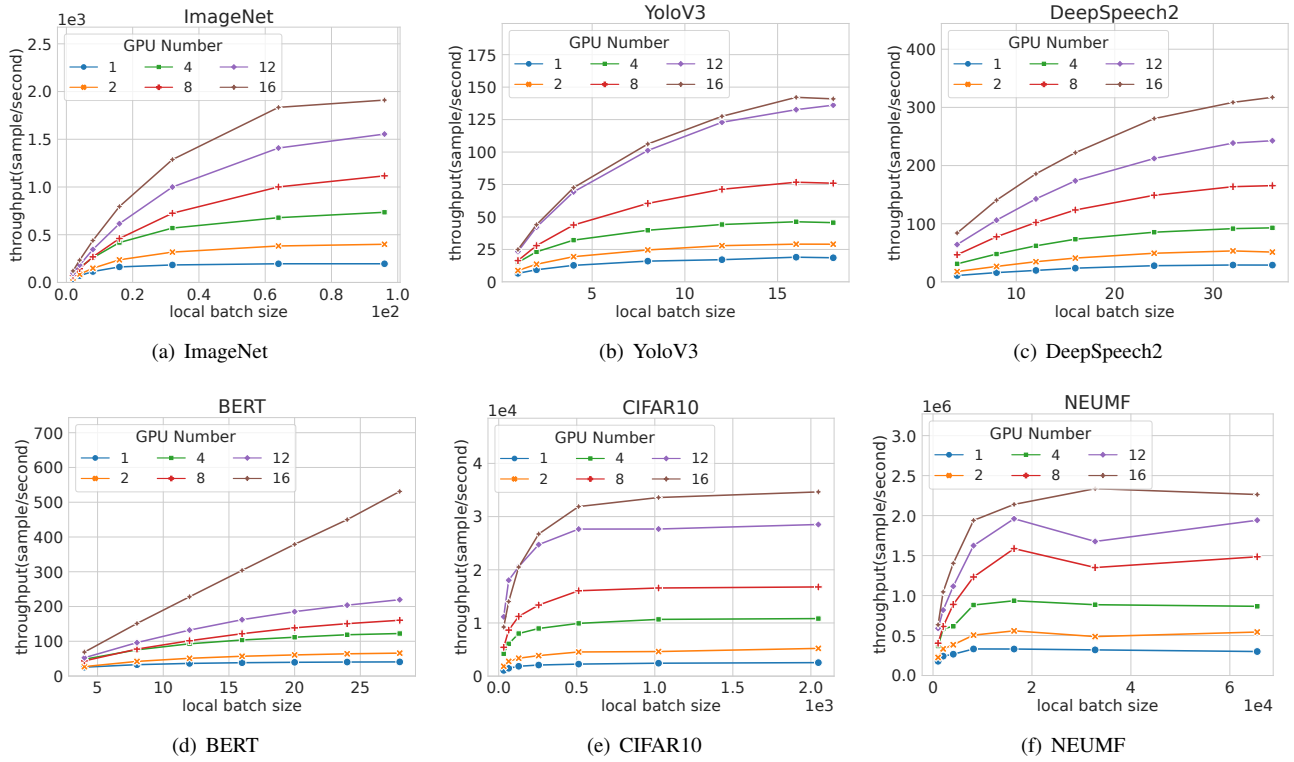


Figure 2. System throughput for all DL models in our experiments, as measured using a 4-server cluster each with 4 NVIDIA 2080Ti GPU. Each sub-figure shows the values of different resource and training batch size settings for each model.

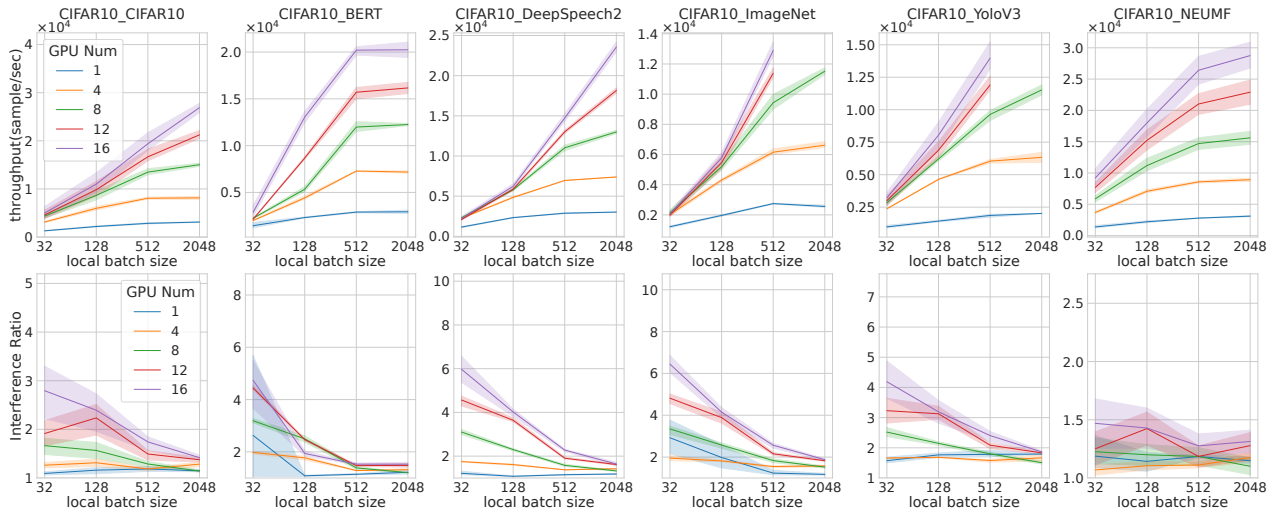


Figure 3. TOP: System throughput of difference DL models paired with CIFAR10 to share the same set of GPUs. BOTTOM: the interference ratio ξ for different DL models and resource and training settings.

V. SOLUTION

We note that Problem (15) presents an integer non-convex program with packing and covering constraints, which is NP-hard. Given these challenges, we opt to explore a heuristic approach that provides a provable local optimum guarantee for a job pair that shares GPUs either completely or partially.

In this section, we describe our solution to address the problem formulated in Section IV. The solution comprises

two parts. Firstly, we address the simple case of two jobs: one running on the GPUs while the other awaits scheduling. It is important to note that concurrent execution on a GPU may degrade overall performance if interference is significant. Thus, we must decide whether the jobs should share GPUs and when to launch the waiting one. This gives rise to **Theorem 1**, which forms the core of our solution by providing a feasible solution when cluster resources are insufficient. Secondly, we

introduce our scheduling algorithm SJF-BSBF (shortest job first with best sharing benefit first), built upon **Theorem 1** and the shortest job first strategy. By judiciously selecting job pairs that benefit from GPU sharing, even acting in a non-preemptive manner, SJF-BSBF reduces job queuing time while avoiding scenarios where sharing may detrimentally impact overall performance.

A. Scheduling One Job Pair

We assume that all the tasks of a DL job are assigned to a fixed set of GPUs during its execution. Before we design the scheduling algorithm, each new-arriving DL job should be placed to a certain set of intra-node or inter-node processors, which is called job placement.

Assume that there is a new job A sharing the GPUs occupied by the existing job B , and their execution time under concurrent execution is respectively

$$\hat{t}_A = t_A \xi_A, \quad (16)$$

$$\hat{t}_B = t_B \xi_B, \quad (17)$$

and κ is the inserting time. We have the following theorem.

Theorem 1 The shortest JCT of the above job pair is achieved by either sequentially executing them ($\kappa = t_A i_A$) or simultaneously invoking them concurrently $\kappa = 0$.

Proof. Case 1: If $\hat{t}_A i_A \geq \hat{t}_B i_B$, then

$$T_A = \hat{t}_B i_B + t_A \times \left(i_A - \frac{\hat{t}_B i_B}{\hat{t}_A} \right), \quad (18)$$

$$T_B = \hat{t}_B i_B. \quad (19)$$

The average time is

$$\bar{T} = (T_A + T_B)/2, \quad (20)$$

$$= \hat{t}_B i_B + \frac{t_A i_A}{2} - \frac{\hat{t}_B i_B}{2 \xi_A}. \quad (21)$$

Case 2: If $\hat{t}_A i_A < \hat{t}_B i_B$, then

$$T_A = \kappa + \hat{t}_A \times \left(i_A - \frac{\kappa}{\hat{t}_A} \right), \quad (22)$$

$$T_B = \kappa + \hat{t}_A \times \left(i_A - \frac{\kappa}{\hat{t}_A} \right) + t_B \times \left(i_B - \frac{\hat{t}_A \times \left(i_A - \frac{\kappa}{\hat{t}_A} \right)}{\hat{t}_B} \right). \quad (23)$$

The average time is

$$\bar{T} = (T_A + T_B)/2 \quad (24)$$

$$= \left(\frac{2\xi_B + \xi_A - 2\xi_A \xi_B}{2\xi_B} \right) \kappa + \left(1 - \frac{1}{2\xi_B} \right) \hat{t}_A i_A + \frac{1}{2} t_B i_B. \quad (25)$$

If $2\xi_B + \xi_A - 2\xi_A \xi_B > 0$, it is an monotonically increasing function with respect to κ . The minimum value is achieved at $\kappa = 0$, which indicates that one should start the new job immediately. Otherwise, it is an monotonically increasing function with respect to κ . The minimum value is achieved at $\kappa = t_A i_A$, which indicates that overlapping two jobs degrade the overall performance. \square

In practice, evaluating the conditions for the best solution is the same as directly comparing the fully overlapped time and the fully non-overlapped time in terms of time cost.

B. Scheduling Multiple DL Jobs

One critical challenge in addressing Problem (15) is the allocation of GPUs when all GPUs in the cluster are occupied by existing jobs, and a new job arrives. One needs to determine 1) which job to share resources with the new arrival, 2) deciding when to initiate the new job. Our goal is to develop a heuristic efficient online scheduling algorithm for it.

1) **Basic Idea:** We propose an online scheduling algorithm called SJF-BSBF (smallest job first with best sharing benefit first). Algorithm 1 describes the steps of SJF-BSBF. The intuition behind Algorithm 1 has three points. 1) As for job priority, the overall framework is based on the shortest job first (SJF) strategy, as tackled by Lines 1-2. This size-based heuristic strategies determine the job priority according to their used GPU numbers. We apply SJF since it performs well most of time for online scheduling problems [13]. 2) As for GPU allocation, since the case of scheduling two jobs concurrently running on the same GPUs (wholly or partially) is considered in our paper, once the free GPU number is not enough to execute the job, we manage to look for those already occupied by the running jobs to schedule the new one. This is the core logic of SJF-BSBF and handled by Lines 3-19. 3) In the point of 2), for each job pair, we should also decide the batch size of the new job for gradient accumulation that not only exceeds the GPU memory size but also achieves the shortest JCT of scheduling the job pair. This corresponds to Line 11.

2) **GPU Allocation:** Given a job J_k that needs G_{J_k} GPUs, we should decide a set of GPUs to schedule it. The classical heuristic algorithms include First-Fit (FF) [33] and List-Scheduling (LS) [33]. In Algorithm 1, Lines 3-19 present the step of choosing the GPUs. First, if there are enough GPUs to execute J_k , we select the top- k GPU in \mathcal{G}_{free} to make them as colidated on the nodes as possible (Lines 6-7). Second, notice that we allow at most two jobs to concurrently run on the same GPUs. Once the free GPU number is smaller than the request of J_k , we attempt to seek those GPUs that are already occupied by one job (Lines 10-17). We scan G_{OJ} and determine the best concurrent running setting of the running job and J_k , including the batch size of J_k and whether to let them share the GPUs, using Algorithm 2 introduced later. We add those pairs that can benefit from the sharing strategy (Lines 10-13). Then we sort \mathcal{J}_{share} by the JCT of the job pair in ascending order (Line 14). Finally, we pick up the GPUs from those candidate jobs until the total number can fulfill the request of J_k (Lines 15-17). Notice that we do not pick the free GPUs at first for this case to save resources because the completion time of J_k is determined by those shared GPUs.

3) **Batch Size Scaling:** In Algorithm 2, given a running job J_{run} and a new job J_k ready to be scheduled, we present how to adaptively adjust the batch size for J_k to achieve the shortest average JCT of these two jobs. Notice that we do not adjust the batch size of the running job to reduce the complexity of

Algorithm 1 Shortest Job First with Best Sharing Benefit First (SJF-BSBF)

Input: The pending job list $\mathcal{J}_{pending}$ to allocate GPUs at the current scheduling time point. L_k is the expected remaining time of J_k , calculated by $t_{iter}^j \times I_k$. \mathcal{G}_{OJ} denotes the GPU set occupied by at least one job. \mathcal{J}_{share} denotes the candidate job set for concurrent execution.

Output: $\mathcal{G}(J_k)$, The GPU sets of each job J_k in $\mathcal{J}_{pending}$.

```
1: Sort  $\mathcal{J}_{pending}$  by  $L_k$  in ascending order.
2: for  $J_k$  in  $\mathcal{J}_{pending}$  do
3:    $\mathcal{G}(J_k) \leftarrow \emptyset$ .
4:    $\mathcal{G}_{free} \leftarrow$  GPUs that hold no job.
5:    $\mathcal{G}_{OJ} \leftarrow$  GPUs that hold one job.
6:   if  $|\mathcal{G}_{free}| \geq G_{J_k}$  then
7:      $\mathcal{G}(J_k) \leftarrow$  the top- $G_{J_k}$  GPUs in  $\mathcal{G}_{free}$ 
8:   else
9:     if  $|\mathcal{G}_{free}| + |\mathcal{G}_{OJ}| \geq G_{J_k}$  then
10:      for  $g$  in  $\mathcal{G}_{OJ}$  do
11:        Get  $SF, b, t$  using Algorithm 2.
12:        Add  $J_g$  to  $\mathcal{J}_{share}$  if SF is True.
13:      end for
14:      Sort  $\mathcal{J}_{share}$  by  $t$  in ascending order.
15:      for  $J$  in  $\mathcal{J}_{share}$  do
16:        Add  $\mathcal{G}_J$  to  $\mathcal{G}_{J_k}$  until  $|\mathcal{G}_{J_k}| \geq G_{J_k}$ .
17:      end for
18:    end if
19:  end if
20: end for
```

Algorithm 2 Batch Size Scaling with Best Sharing Benefit

Input: A given job J_k to allocate GPUs. The user's requested batch size B_k . t_{share} represents the JCT of the best sharing configuration of two jobs.

Output: The sharing configuration denoted by $\overline{SF}, \bar{b}, \bar{t}$. \overline{SF} indicates whether to share the GPU for the new job.

```
1:  $b \leftarrow B_{J_k}$ 
2:  $\bar{b} \leftarrow B_{J_k}$ 
3:  $\bar{t} \leftarrow$  a large number
4:  $\overline{SF} \leftarrow False$ 
5: while  $[b] \neq 1$  do
6:   Get  $SF$  and  $t_{share}$  according to Theorem 1.
7:   if  $t_{share} \leq \bar{t}$  then
8:      $\bar{t} \leftarrow t$ 
9:      $\bar{b} \leftarrow b$ 
10:     $\overline{SF} \leftarrow SF$ 
11:  end if
12:   $b \leftarrow b/2$ 
13: return  $\overline{SF}, \bar{b}, \bar{t}$ .
14: end while
```

the scheduling system. We search the batch size in the range $[1, B_{J_k}]$ with a step of power two (Lines 5 and 12). For each candidate batch size, we use **Theorem 1** to obtain the best configuration of scheduling the job pair, including the flag of whether to let them share GPUs (SF) and the JCT (Line 6). Then we record that configuration if better (Lines 7-11). Notice that it is possible that the new job J_k may not be scheduled immediately and put back to the pending job pool if the final \overline{SF} is *False*, indicating that running the job pair concurrently is not optimal.

4) **Time complexity of SJF-BSBF:** The time consumption of SJF-BSBF is primarily attributed to searching the GPU set for a pending job to be shared when there is insufficient resource (Lines 9 to Line 18 in Algorithm 1). Initially, a for loop (Line 10) scans all GPUs with one job, iterating $|\mathcal{G}(OJ)|$ times. Subsequently, each iteration executes Algorithm 2 to determine the time point to initiate GPU sharing as well as the appropriate batch size, with a time complexity of $\theta(\log_2(B_{J_k}))$. Lastly, after collecting candidate jobs for sharing GPUs, sorting the list in ascending order to select those with the shortest Job Completion Time (JCT) requires $\theta(|\mathcal{J}_{share}| \log_2(|\mathcal{J}_{share}|))$. Consequently, the time complexity for scheduling a job is $\theta(|\mathcal{G}(OJ)| \log_2(B_{J_k}) + |\mathcal{J}_{share}| \log_2(|\mathcal{J}_{share}|))$. In our system implementation on a 16-GPU cluster, the overhead of periodically scheduling those waiting jobs is negligible, averaging below 0.02 seconds for each operation.

VI. PERFORMANCE EVALUATION

A. Experimental Setup

Cluster configurations: We first conduct physical experiments on a cluster of four servers. Each server is equipped with an Intel Xeon CPU E5-2670 and four Nvidia GeForce 2080 Ti GPUs. The network is configured with Fat-Tree topology with 10 Gbps connected to a 100-Gbps switch. All experiments are performed in the environment of Ubuntu 20.04, PyTorch 1.18, CUDA 11.2 and OpenMPI 4.0. Based on the data measured on the physical environment, we then conduct simulation experiments to resemble the physical cluster configuration and test large scale of clusters and job traces. To evaluate the performance of SJF-BSBF in a large-scale cluster (16 servers each with 4 GPUs) with long-term traces, we also implement a simulator to record job events and resource usage. All experiment results without explicit comments are derived from the simulation.

Baselines: We consider the following baselines.

1) *First-In-First-Out (FIFO)*: a traditional but popular policy adopted by several well-known cluster management systems, such as Yarn and Kubernetes. However, it usually performs poor due to its runtime-agnostic scheduling paradigm. Picks the top- G_j GPU with least execution time first.

2) *Shortest Job First (SJF)*: an ideal policy to minimize the average JCT without preemption by prioritizing short-term jobs to overcome HOL blocking. It is impractical as it requires perfect job information which is impossible to attain.

3) *Tiresias* [13]: a preemptive policy that prioritizes least attained service jobs (i.e., consumed GPU numbers and training iterations). Under this policy, it helps short-term jobs escape from resource starvation and finish earlier without any prior information.

4) *Shortest Job First with First Fit Sharing (SJF-FFS)*: a sharing policy built upon SJF. It is similar to our proposed SJF-BSBF except that it does not search the best sharing configuration as SJF-BSBF but allocates the job to those GPUs that only have one job in a first fit manner if the free GPUs are not sufficient for the new job. This policy is a comparison baseline to validate the effectiveness of wisely sharing the GPUs in SJF-BSBF.

5) *Pollux* [15]: the state-of-the-art elastic scheduler that adaptively adjust the GPU resources for each job to optimize the overall job performance as well as resource utilization. As explained in [20], Pollux cannot guarantee no accuracy degradation for all models as it allows the scheduler to tune the training batch size, while our SJF-BSBF applies gradient accumulation to attain the same convergence as the original user specific batch size setting.

For physical experiments, we compare our SJF-BSBF with FIFO, SJF and Tiresias to demonstrate the advantages of resource sharing over those exclusive-mode policies. For simulation experiments, we also add Pollux, one of the state-of-the-art elasticity-based scheduler, to compare the sharing-based and the elasticity-based policies.

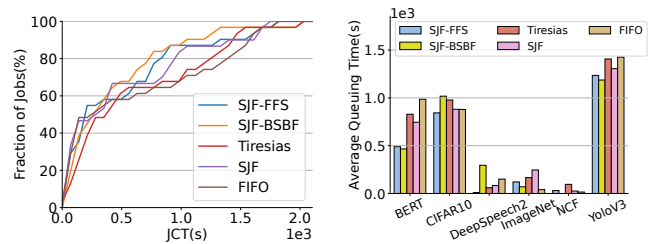
Workload Settings: We generate the workload similar to the Microsoft job trace [3]. More details about the Microsoft trace can be found in [3] and Appendix of [13]. For the physical experiments, considering that our testbed only has 4 nodes with 16 GPUs, we generate totally 30 DDL jobs by scaling down the original job trace. As job characteristics, such as the number of GPUs and the training iterations, we mostly follow the distributions of the real trace: 20 jobs using no more than 8 GPUs and 10 jobs using 12 or 16 GPUs. The training iteration of jobs varies from 100 to 5000. For the simulation experiments, we mainly follow the settings of Pollux [15]. We randomly sample 240 jobs from the busiest period in the deep learning cluster traces published by Microsoft [3] and also annotate six DL tasks (BERT, CIFAR10, DeepSpeech2, ImageNet, NCF and YoloV3) used in Pollux to them. The settings of GPU numbers and training iterations also follow those of Pollux.

B. Experimental Results on a Physical Cluster

JCT Improvements: Figure 4(a) demonstrates the JCT distributions of the baseline workload using different scheduling policies. Nearly 80% of jobs have no more than 0.75 hour of JCTs using our SJF-BSBF, while other algorithms only have less than 70%. SJF-BSBF generally achieves the best performance. In Table II, it is reported that SJF-FFS and SJF-BSBF, which allows the GPUs to be shared among jobs, have considerable performance improvements over other policies. In particular, SJF-BSBF achieves a 27% lower average JCT than Tiresias. Besides, instead of allowing GPU sharing in a

greedy manner, SJF-BSBF can adaptively select the best job combination as well as the scheduling point to avoid those job pairs that may bring down the overall performance, which outperforms SJF-FFS by 9% in terms of JCT.

Job Queuing Delay: Figure 4(b) shows the average queuing time of different scheduling policies on different DDL job models. First, the queuing time of SJF-BSBF is generally lower than those heuristic policies with the exclusive GPU mode. For the model BERT, SJF-BSBF reduces the queuing time by nearly 44% compared to Tiresias. Second, since SJF-FFS allows the jobs to share the GPUs in an aggressive manner, it generally has the lowest queuing time. However, as reported in Figure 4(a) and Table II, it usually leads to a longer JCT since some job pairs have a high interference ratio and subsequently hurt the overall performance.



(a) JCT distributions of different scheduling policies in the physical experiments. (b) Average queuing time of different scheduling policies in the physical experiments.

Figure 4. Performance of different policies in physical experiments.

Table II
THE MAKESPAN AND AVERAGE JCT RUN BY PHYSICAL EXPERIMENTS.

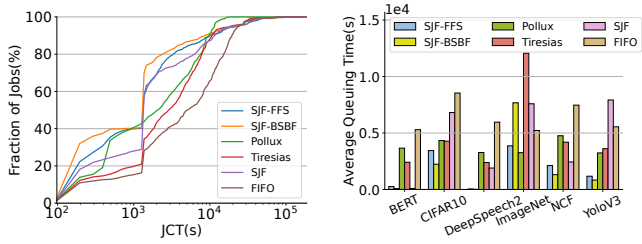
Policy	Makespan (seconds)	Average JCT (seconds)
FIFO	2317	662.6
SJF	2319	609.55
Tiresias	2398	664.73
SJF-FFS	2176	530.36
SJF-BSBF	2129	483.16

C. Experimental Results on Large-Scale Simulations

To verify the fidelity of our simulator, we also compare the results of physical experiments with simulations. We observe that the simulator can achieve the realistic experimental performance within 5% relative percentage errors on both makespan and average JCT. This confirms the high fidelity of our simulator.

JCT Improvements: We first compare the JCTs of different scheduling policies on the standard simulation workload. In Figure 5(a), it is evident that SJF-BSBF outperforms other policies. Nearly 40% of jobs of SJF-BSBF achieves lower than 500 seconds of JCTs, reducing the average JCT of the shortest 40% jobs by 37% than Pollux. This demonstrates the preemption-free policy can even obtain better performance than the preemptive policy, such as Tiresias and Pollux.

Tables III and IV present the performance of different scheduling policies for 240 jobs and 480 jobs, respectively.



(a) JCT distributions of different scheduling policies in the simulation experiments. (b) Average queuing time of different scheduling policies in the simulation experiments.

Figure 5. Performance of different policies in simulation experiments.

Jobs are characterized based on their requested number of GPUs, with those requiring more than 4 GPUs considered large, and others small. For the workload of 240 jobs, SJF-BSBF demonstrates slightly better performance than the advanced policy Pollux. While large jobs under SJF-BSBF may experience longer JCTs than Pollux due to GPU sharing overhead, small jobs benefit significantly by potentially sharing GPUs with large jobs, resulting in markedly shorter queuing times compared to other preemption-free policies. This advantage is further accentuated as the number of jobs increases. In Table IV with 480 jobs, SJF-BSBF enhances the average JCT by nearly 3 times compared to Pollux, primarily attributable to the reduction in queuing time for small jobs. Moreover, SJF-BSBF outperforms SJF-FFS by reducing the average JCT and queuing time by 17% and 5.5%, respectively.

Table III
PERFORMANCE OF LARGE-SCALE AND SMALL-SCALE JOBS BY SIMULATION. (240 JOBS)

Metrics (hrs)	Policy	All Jobs	Large Jobs	Small Jobs
Average JCT	FIFO	2.34	3.92	2.13
	SJF	1.25	3.50	0.94
	Tiresias	1.51	3.48	1.23
	Pollux	1.04	1.96	0.91
	SJF-FFS	1.23	4.29	0.81
	SJF-BSBF	1.01	3.38	0.68
Average Queuing Time	FIFO	1.65	2.17	1.58
	SJF	0.56	1.76	0.39
	Tiresias	0.81	1.73	0.68
	Pollux	1.00	1.21	0.97
	SJF-FFS	0.18	0.98	0.07
	SJF-BSBF	0.14	0.89	0.03

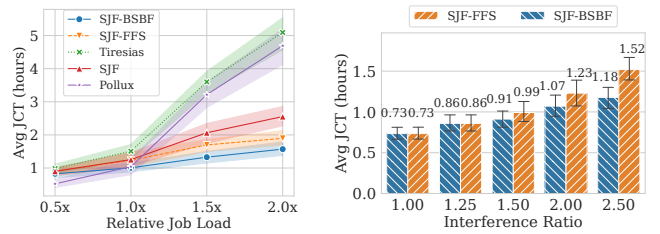
Job Queuing Delay: Figure 5(b) presents a comparison of the average queuing time among different scheduling policies for various DDL job tasks in simulation. Notably, the GPU sharing policies, namely SJF-BSBF and SJF-FFS, consistently yield lower queuing times compared to heuristic policies operating in exclusive GPU mode. Additionally, preemptive policies such as Tiresias and Pollux often exhibit longer queuing times attributable to job migration.

Sensitivity to job load: We compare the performance of our SJF-BSBF to other existing policies for increasing workload intensity in terms of job submission frequencies. We scale the baseline workload of 240 jobs by $0.5\times \sim 2\times$, ranging from

Table IV
PERFORMANCE OF LARGE-SCALE AND SMALL-SCALE JOBS BY SIMULATION. (480 JOBS)

Metrics (hrs)	Policy	All Jobs	Large Jobs	Small Jobs
Average JCT	FIFO	7.52	10.06	7.08
	SJF	2.55	7.00	1.90
	Tiresias	5.09	8.25	4.59
	Pollux	4.69	6.03	4.51
	SJF-FFS	1.89	8.12	0.99
	SJF-BSBF	1.57	6.13	0.88
Average Queuing Time	FIFO	0.73	4.06	0.21
	SJF	1.87	5.35	1.35
	Tiresias	4.41	6.60	4.04
	Pollux	4.41	5.03	4.31
	SJF-FFS	0.73	4.06	0.21
	SJF-BSBF	0.69	3.62	0.21

120 jobs to 480 jobs. Figure 6(a) shows the results. An interesting phenomenon is that Pollux can have better performance than other policies when the job workload intensity is low. Pollux is more suitable for lighter workload intensity because its adaptive job batch size and resource scaling techniques are limited when clusters are overloaded, which meets the findings in [16], [20]. However, when the workload increases, the GPU resources are rather insufficient so that Pollux cannot benefit from this strategy. Across all job workloads, our SJF-BSBF maintains relatively low improvements over other baseline policies since it allows the jobs to share the GPUs to shrink the job queuing time.



(a) Varying the workloads. (b) Varying the interference ratios.

Figure 6. Effects of various workloads and interference ratios.

Impact of Different Interference Ratios: To evaluate the impact of different interference ratios on our GPU sharing policies, SJF-FFS and SJF-BSBF, we artificially inject various values for all the jobs sharing the same GPUs in the baseline simulation workload. Figure 6(b) shows the results. When the ratio is small ($\xi \leq 1.25$), which is the ideal scenario that sharing GPUs brings negligible overhead, SJF-BSBF tends to allow all the available sharing decisions as SJF-FFS, which results in the same performance. However, when the GPU sharing leads to severe slowdowns for the running jobs, our SJF-BSBF can get rid of those job pairs that may hurt the overall performance in SJF-FFS, which reduces the average JCT by 8%~13% when ξ ranges from 1.5 to 2.0.

VII. CONCLUSION

In this paper, we delve into resource scheduling for DL jobs in a multi-tenant GPU cluster, where we harness GPU sharing

capabilities to diminish job queuing time and enhance overall performance. We begin by formulating a DL scheduling model that accounts for GPU sharing among various jobs and employs gradient accumulation to surmount memory limitations while maintaining the job training accuracy. We then derive the optimal solution to schedule a job pair on the same set of GPUs and further design an efficient heuristic scheduling algorithm upon it to unleash the potential of GPU sharing in reducing the job queuing time and avoid serious interference with the running jobs. Extensive experiments, including physical implementations and simulations, were conducted to demonstrate the effectiveness of SJF-BSBF. Our findings reveal that the non-preemptive SJF-BSBF surpasses advanced preemptive policies like Tiresias and Pollux by leveraging GPU sharing techniques. Furthermore, identifying appropriate sharing settings is pivotal in mitigating severe degradation cases induced by high interference.

ACKNOWLEDGMENTS

This research was supported by the National Natural Science Foundation of China (No. 62302126, No. 62302123), the Shenzhen Science and Technology Program (No. RCBS20221008093125065, No. JSGGKQTD20221101115655027, No. JCYJ20220818102414030, No. KJZD20230923115113026, No. KJZD20230923114213027), and Guangdong Provincial Key Laboratory of Novel Security Intelligence Technologies (2022B1212010005).

REFERENCES

- [1] Y. LeCun, Y. Bengio, and G. Hinton, "Deep Learning," *nature*, vol. 521, no. 7553, p. 436, 2015.
- [2] J. Dean, G. Corrado, R. Monga, K. Chen, M. Devin, M. Mao, M. aurelio Ranzato, A. Senior, P. Tucker, K. Yang, Q. V. Le, and A. Y. Ng, "Large Scale Distributed Deep Networks," in *Advances in Neural Information Processing Systems 25*, 2012, pp. 1223–1231.
- [3] M. Jeon, S. Venkataraman, A. Phanishayee, J. Qian, W. Xiao, and F. Yang, "Analysis of large-scale multi-tenant gpu clusters for dnn training workloads," *arXiv preprint arXiv:1901.05758*, 2019.
- [4] V. Jalaparti, P. Bodik, I. Menache, S. Rao, K. Makarychev, and M. Caesar, "Network-aware scheduling for data-parallel jobs: Plan when you can," in *Proceedings of the 2015 ACM Conference on Special Interest Group on Data Communication*, ser. SIGCOMM, 2015, pp. 407–420.
- [5] F. Giroire, N. Huin, A. Tomassilli, and S. Pérennes, "When Network Matters: Data Center Scheduling with Network Tasks," in *IEEE INFOCOM 2019 - IEEE Conference on Computer Communications*, April 2019, pp. 2278–2286.
- [6] A. Tumanov, T. Zhu, J. W. Park, M. A. Kozuch, M. Harchol-Balter, and G. R. Ganger, "Tetrisched: Global rescheduling with adaptive plan-ahead in dynamic heterogeneous clusters," in *Proceedings of the Eleventh European Conference on Computer Systems*, ser. EuroSys, 2016.
- [7] Y. Liu, H. Xu, and W. C. Lau, "Online job scheduling with resource packing on a cluster of heterogeneous servers," in *IEEE Conference on Computer Communications (INFOCOM)*, 2019, pp. 1441–1449.
- [8] C. Chen, X. Ke, T. Zeyl *et al.*, "Minimum Makespan Workflow Scheduling for Malleable Jobs with Precedence Constraints and Lifetime Resource Demands," in *2019 IEEE 39th International Conference on Distributed Computing Systems (ICDCS)*, July 2019.
- [9] X. Mei, X. Chu, H. Liu, Y. Leung, and Z. Li, "Energy efficient real-time task scheduling on cpu-gpu hybrid clusters," in *IEEE INFOCOM 2017 - IEEE Conference on Computer Communications*, May 2017, pp. 1–9.
- [10] H. Yabuuchi, D. Taniwaki, and S. Omura, "Low-latency job scheduling with preemption for the development of deep learning," in *USENIX Conference on Operational Machine Learning (OpML)*, 2019.

- [11] A. Hsu, K. Hu, J. Hung, A. Suresh, and Z. Zhang, "Tony: An orchestrator for distributed machine learning jobs," in *2019 USENIX Conference on Operational Machine Learning (OpML 19)*, 2019, pp. 39–41.
- [12] Y. Peng, Y. Bao, Y. Chen, C. Wu, and C. Guo, "Optimus: An Efficient Dynamic Resource Scheduler for Deep Learning Clusters," in *Proceedings of the Thirteenth EuroSys Conference*, ser. EuroSys '18, 2018.
- [13] J. Gu, M. Chowdhury, K. G. Shin, Y. Zhu, M. Jeon, J. Qian, H. Liu, and C. Guo, "Tiresias: A GPU Cluster Manager for Distributed Deep Learning," in *16th USENIX Symposium on Networked Systems Design and Implementation (NSDI 19)*, 2019, pp. 485–500.
- [14] D. Narayanan, K. Santhanam, F. Kazhmiaka, A. Phanishayee, and M. Zaharia, "Heterogeneity-Aware cluster scheduling policies for deep learning workloads," in *14th USENIX Symposium on Operating Systems Design and Implementation (OSDI 20)*, Nov. 2020, pp. 481–498.
- [15] A. Qiao, S. K. Choe, S. J. Subramanya, W. Neiswanger, Q. Ho, H. Zhang, G. R. Ganger, and E. P. Xing, "Pollux: Co-adaptive cluster scheduling for goodput-optimized deep learning," in *15th USENIX Symposium on Operating Systems Design and Implementation (OSDI 21)*. USENIX Association, Jul. 2021, pp. 1–18.
- [16] S. Agarwal, A. Phanishayee, and S. Venkataraman, "Blox: A modular toolkit for deep learning schedulers," in *Proceedings of the Nineteenth European Conference on Computer Systems*, ser. EuroSys '24, 2024.
- [17] W. Xiao, R. Bhardwaj, R. Ramjee, M. Sivathanu, N. Kwatra, Z. Han, P. Patel, X. Peng, H. Zhao, Q. Zhang, F. Yang, and L. Zhou, "Gandiva: Introspective Cluster Scheduling for Deep Learning," in *13th USENIX Symposium on Operating Systems Design and Implementation (OSDI 18)*, 2018, pp. 595–610.
- [18] G. Lim, J. Ahn, W. Xiao, Y. Kwon, and M. Jeon, "Zico: Efficient GPU memory sharing for concurrent DNN training," in *2021 USENIX Annual Technical Conference (USENIX ATC 21)*, Jul. 2021, pp. 161–175.
- [19] P. Yu and C. Mosharaf, "Salus: Fine-Grained GPU Sharing Primitives for Deep Learning Applications," in *Proceedings of the third MLSys Conference*, 2019.
- [20] Q. Hu, M. Zhang, P. Sun, Y. Wen, and T. Zhang, "Lucid: A non-intrusive, scalable and interpretable scheduler for deep learning training jobs," in *Proceedings of the 28th ACM International Conference on Architectural Support for Programming Languages and Operating Systems, Volume 2*, ser. ASPLOS 2023, 2023, p. 457–472.
- [21] M. Yu, Y. Tian, B. Ji, C. Wu, H. Rajan, and J. Liu, "Gadget: Online resource optimization for scheduling ring-all-reduce learning jobs," in *IEEE INFOCOM 2022 - IEEE Conference on Computer Communications*, 2022, p. 1569–1578.
- [22] M. Yu, B. Ji, H. Rajan, and J. Liu, "On scheduling ring-all-reduce learning jobs in multi-tenant gpu clusters with communication contention," in *Proceedings of the Twenty-Third International Symposium on Theory, Algorithmic Foundations, and Protocol Design for Mobile Networks and Mobile Computing*, ser. MobiHoc '22, 2022, p. 21–30.
- [23] Z. Huang, B. Jiang, T. Guo, and Y. Liu, "Measuring the impact of gradient accumulation on cloud-based distributed training," in *2023 IEEE/ACM 23rd International Symposium on Cluster, Cloud and Internet Computing (CCGrid)*, 2023, pp. 344–354.
- [24] Y. Huang, Y. Cheng, A. Bapna, O. Firat, M. X. Chen, D. Chen, H. Lee, J. Ngiam, Q. V. Le, Y. Wu, and Z. Chen, *GPipe: Efficient Training of Giant Neural Networks Using Pipeline Parallelism*, 2019.
- [25] H. Zheng, F. Xu, L. Chen, Z. Zhou, and F. Liu, "Cynthia: Cost-Efficient Cloud Resource Provisioning for Predictable Distributed Deep Neural Network Training," in *2019 48th International Conference on Parallel Processing (ICPP)*, Aug 2019.
- [26] Y. Bao, Y. Peng, and C. Wu, "Deep Learning-based Job Placement in Distributed Machine Learning Clusters," in *IEEE INFOCOM 2019 - IEEE Conference on Computer Communications*, April 2019.
- [27] Z. Hu, J. Tu, and B. Li, "Spear: Optimized Dependency-Aware Task Scheduling with Deep Reinforcement Learning," in *IEEE 39th International Conference on Distributed Computing Systems (ICDCS)*, 2019.
- [28] Q. Weng, W. Xiao, Y. Yu, W. Wang, C. Wang, J. He, Y. Li, L. Zhang, W. Lin, and Y. Ding, "MLaaS in the wild: Workload analysis and scheduling in Large-Scale heterogeneous GPU clusters," in *19th USENIX Symposium on Networked Systems Design and Implementation (NSDI 22)*, Renton, WA, Apr. 2022, pp. 945–960.
- [29] Q. Wang, S. Shi, C. Wang, and X. Chu, "Communication contention aware scheduling of multiple deep learning training jobs," *arXiv preprint arXiv:2002.10105*, 2020.

- [30] T. Hoefler, W. Gropp, R. Thakur, and J. L. Träff, "Toward performance models of mpi implementations for understanding application scaling issues," in *Recent Advances in the Message Passing Interface*, 2010.
- [31] C.-C. Huang, G. Jin, and J. Li, "Swapadvisor: Pushing deep learning beyond the gpu memory limit via smart swapping," in *Proceedings of the Twenty-Fifth International Conference on Architectural Support for Programming Languages and Operating Systems (ASPLOS)*, 2020.
- [32] K. Mahajan, A. Balasubramanian, A. Singhvi, S. Venkataraman, A. Akella, A. Phanishayee, and S. Chawla, "Themis: Fair and efficient GPU cluster scheduling," in *17th USENIX Symposium on Networked Systems Design and Implementation (NSDI 20)*. Santa Clara, CA: USENIX Association, Feb. 2020, pp. 289–304.
- [33] G. L. Stavrinides and H. D. Karatza, "Scheduling multiple task graphs in heterogeneous distributed real-time systems by exploiting schedule holes with bin packing techniques," *Simulation Modelling Practice and Theory*, vol. 19, no. 1, pp. 540 – 552, 2011.